Electronic Supporting Information

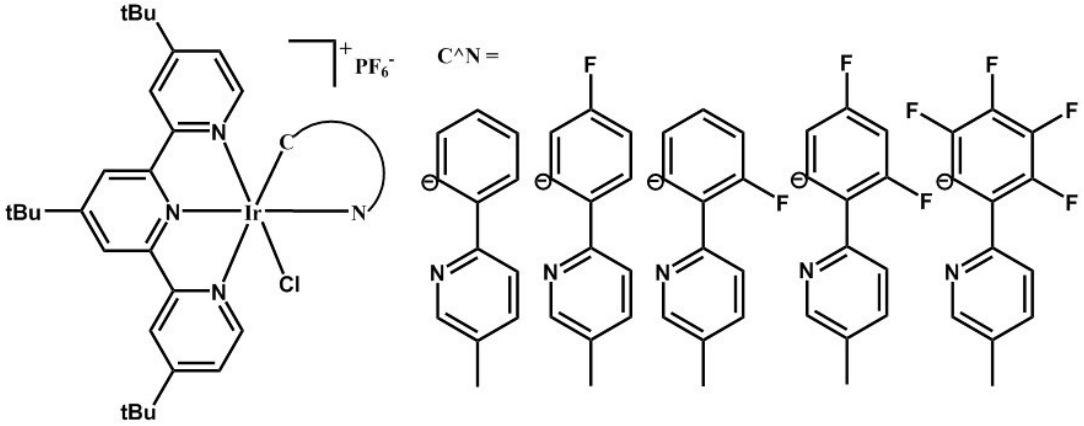

Scheme S1

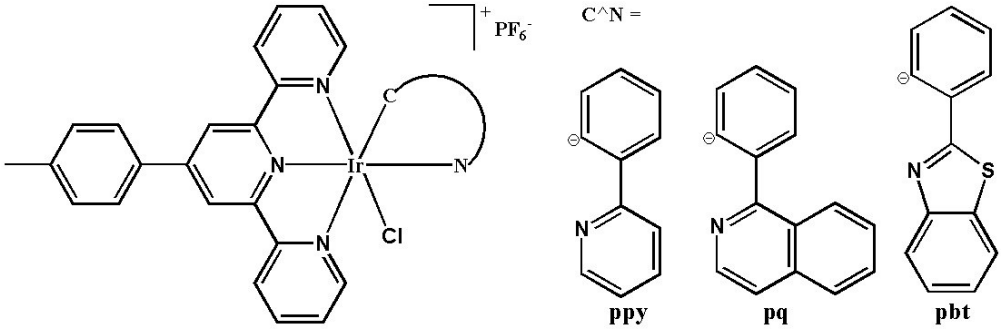

Scheme S2

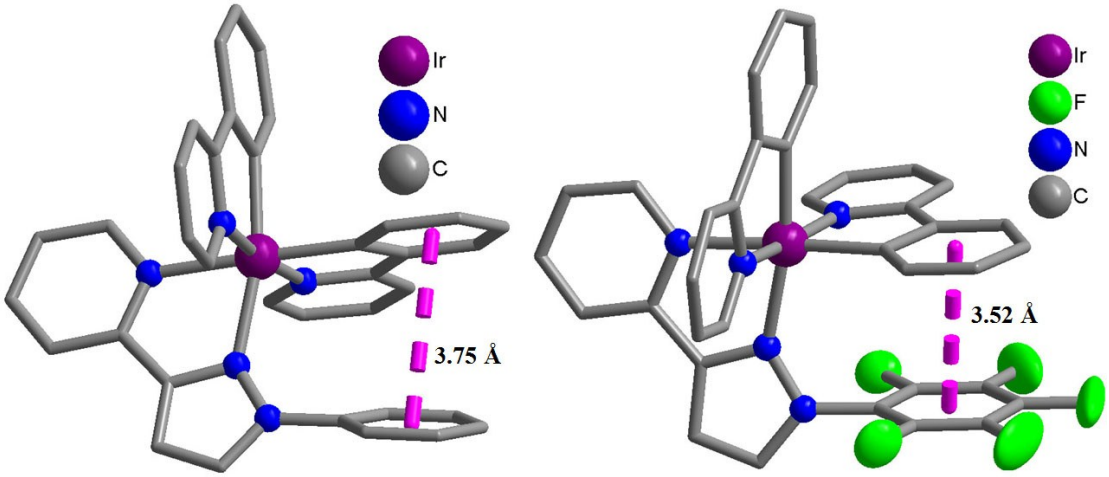

Scheme S3 Molecular structures of $[Ir(ppy)_2(phpzpy)]PF_6$ (left) and $[Ir(ppy)_2(F5phpzpy)]PF_6$ (right) with intramolecular π···π interactions (dashed line).

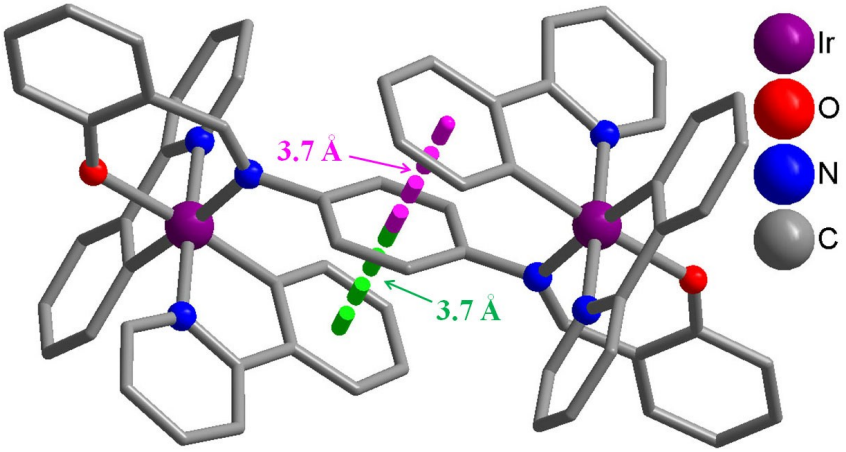

Scheme S4 The molecular structure of $(ppy)_2Ir$-(bsbd)-$Ir(ppy)_2$ showing intramolecular π···π stacking interactions (dashed line)

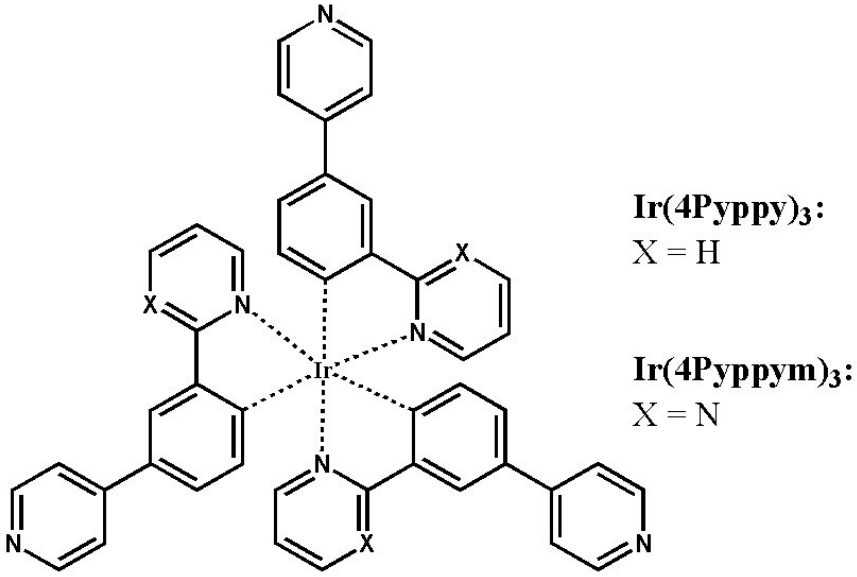

Scheme S5 The molecular structure of $Ir(4Pyppy)_3$ and $Ir(4Pyppym)_3$.

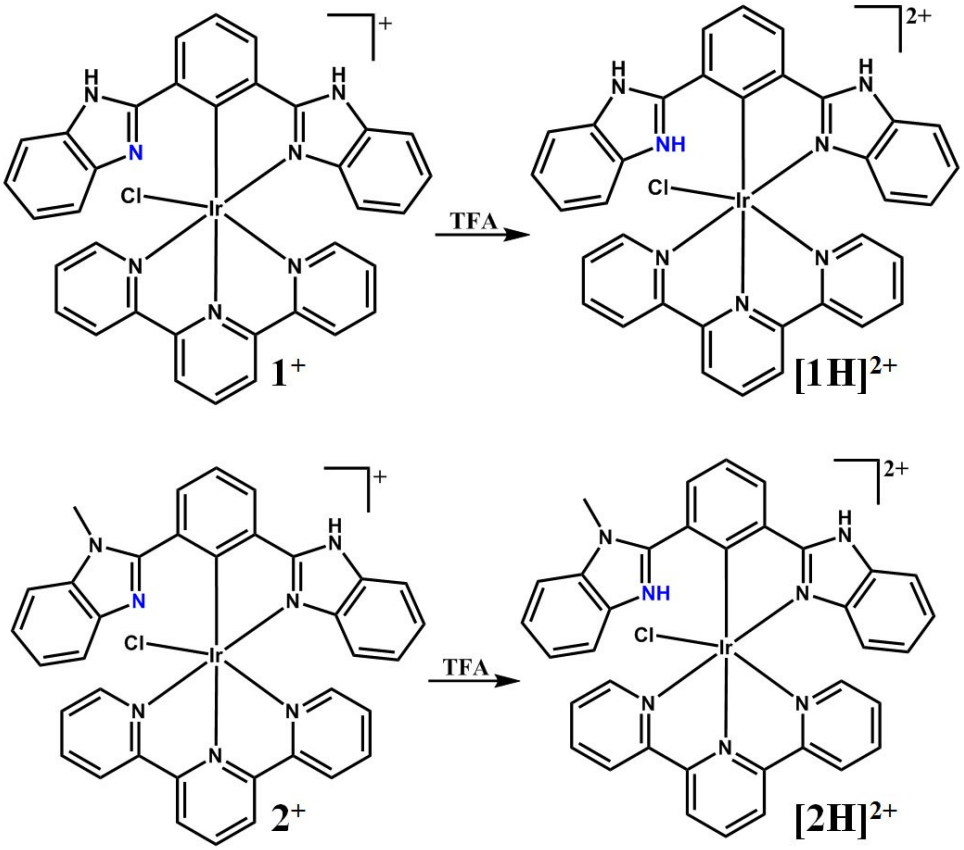

Scheme S6

Table S1 Photophysical properties of **1·PF$_6$**, **2·PF$_6$**, **3·PF$_6$**, bbbiH$_3$, bmbibH and mbibH in CH_3CN at room temperature or in EtOH-MeOH (v/v = 3/1) at 77 K (CH_3CN was degassed for the lifetime measurements of **1·PF$_6$**, **2·PF$_6$** and **3·PF$_6$**).

Compound	Medium	λ_{abs} (nm)	λ_{em} (nm)	Lifetime (μs)	quantum yield
1·PF$_6$	CH_3CN (298 K)	235, 272, 280, 298, 309, 345 and a tail to 540	534	2.39	39.5%
	EtOH-MeOH (77 K)	-	520 and 553	-	-
2·PF$_6$	CH_3CN (298 K)	238, 273, 282, 299, 310, 346 and a tail to 540	536	2.94	66.4%
	EtOH-MeOH (77 K)	-	522 and 555	-	-
3·PF$_6$	CH_3CN (298 K)	236, 270, 281, 299, 309, 346 and a tail to 540	558	1.75	27.0%
	EtOH-MeOH (77 K)	-	538 and 571	-	-
bbbiH$_3$	CH_3CN (298 K)	235, 306	-	-	-
bmbibH	CH_3CN (298 K)	230, 295	-	-	-
mbibH	CH_3CN (298 K)	233, 290	-	-	-

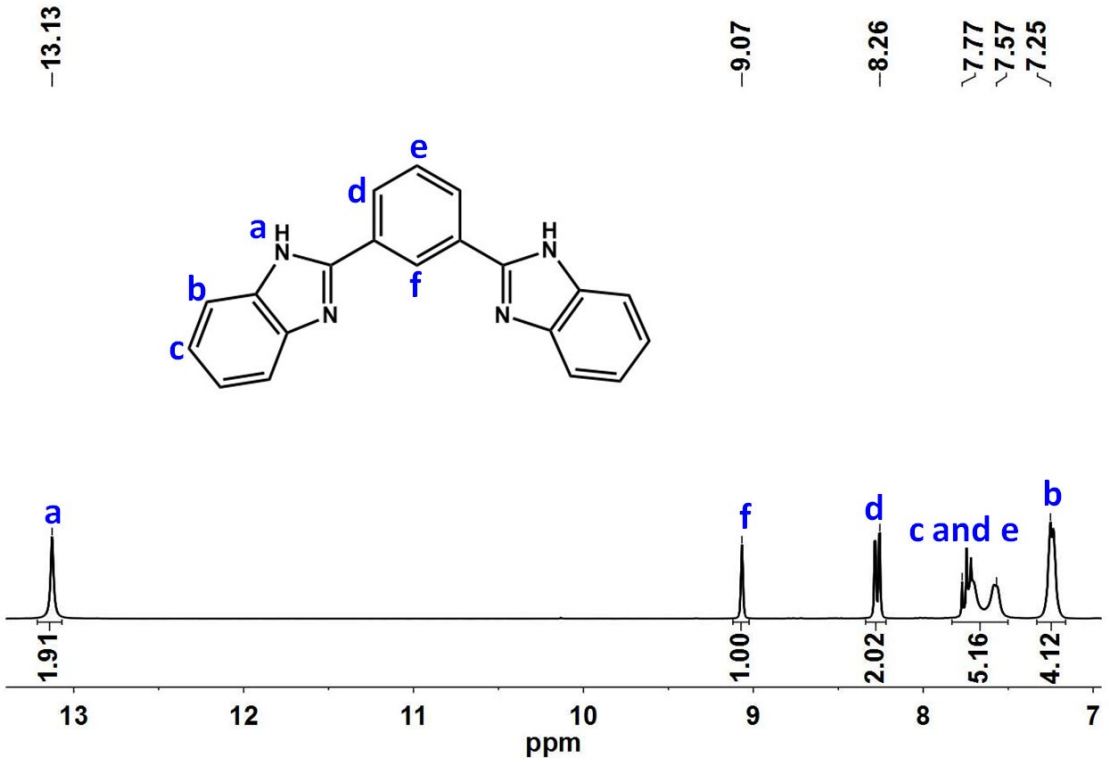

Fig. S1 ^{1}H NMR spectrum of bbibH$_3$ (500 MHz, DMSO-d_6).

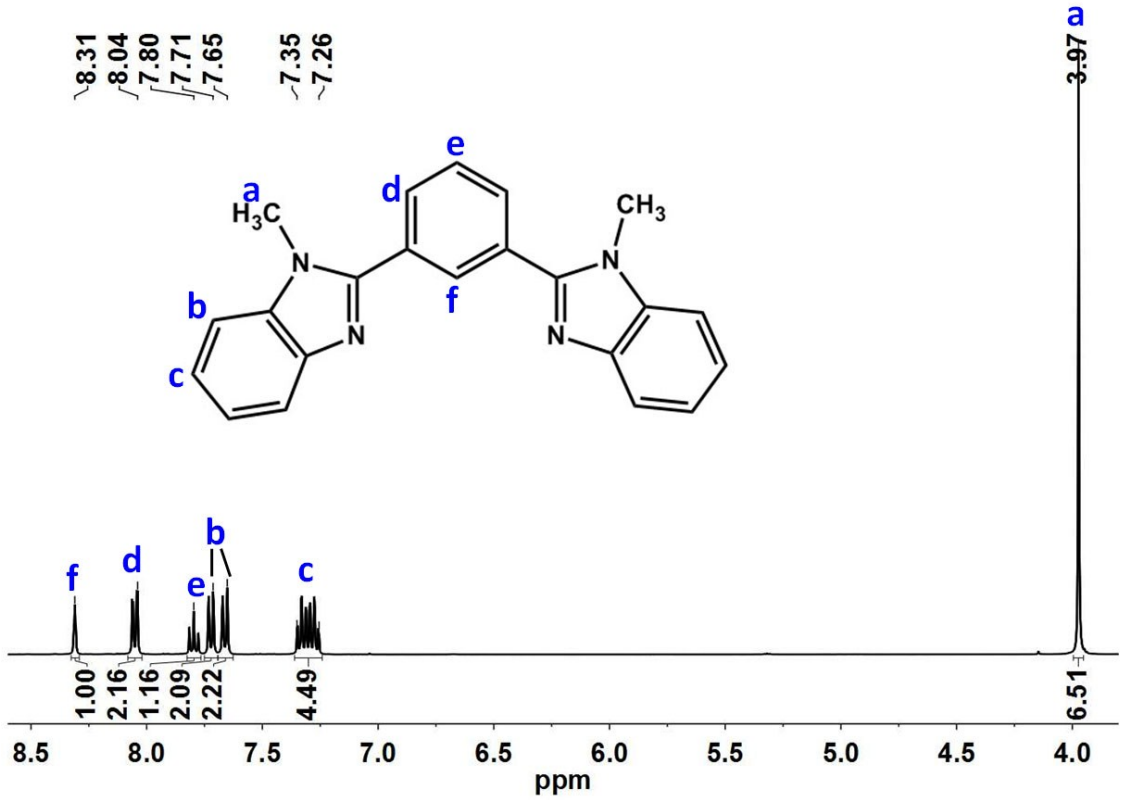

Fig. S2 ^{1}H NMR spectrum of bmbibH (500 MHz, DMSO-d_6).

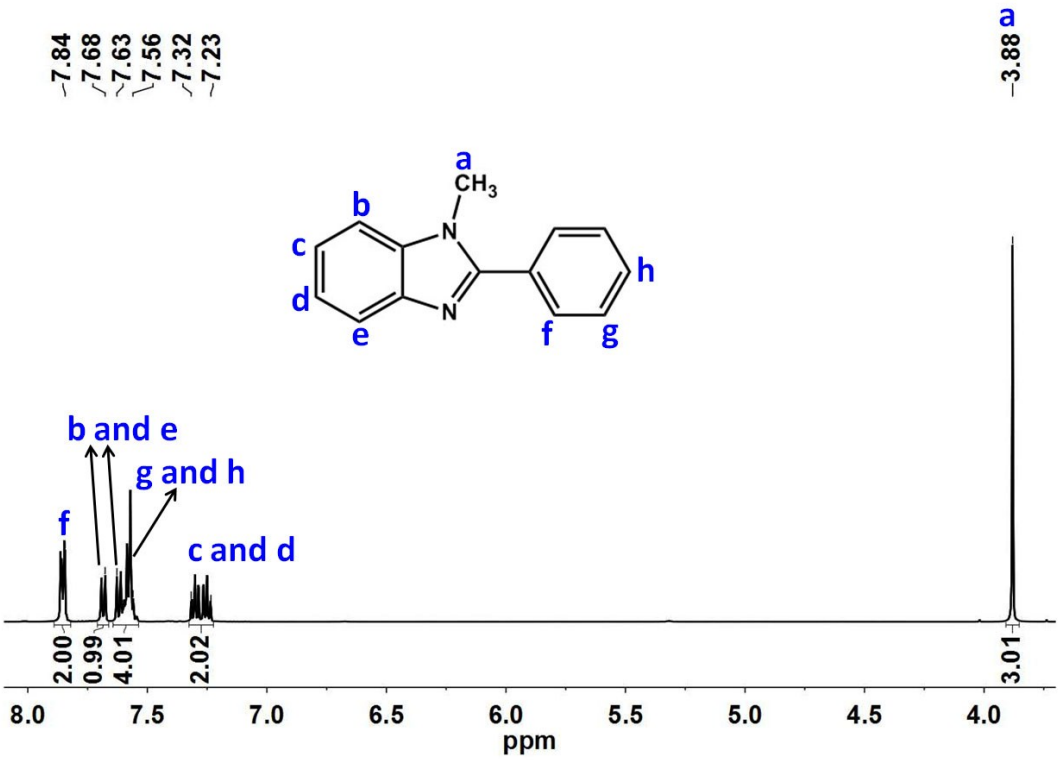

Fig. S3 ^{1}H NMR spectrum of mbibH (500 MHz, DMSO-d_6).

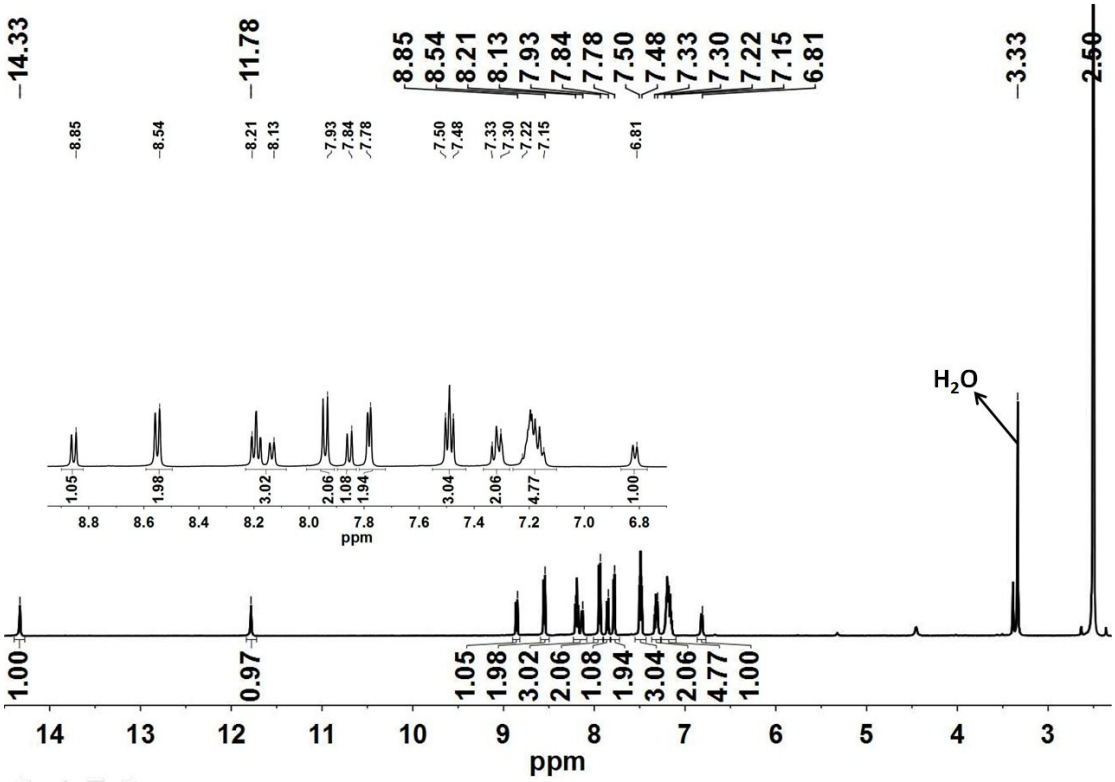

Fig. S4 ^{1}H NMR spectrum of **1·PF$_6$** (500 MHz, DMSO-d_6). The signal at 3.33 ppm are from H_2O, respectively.

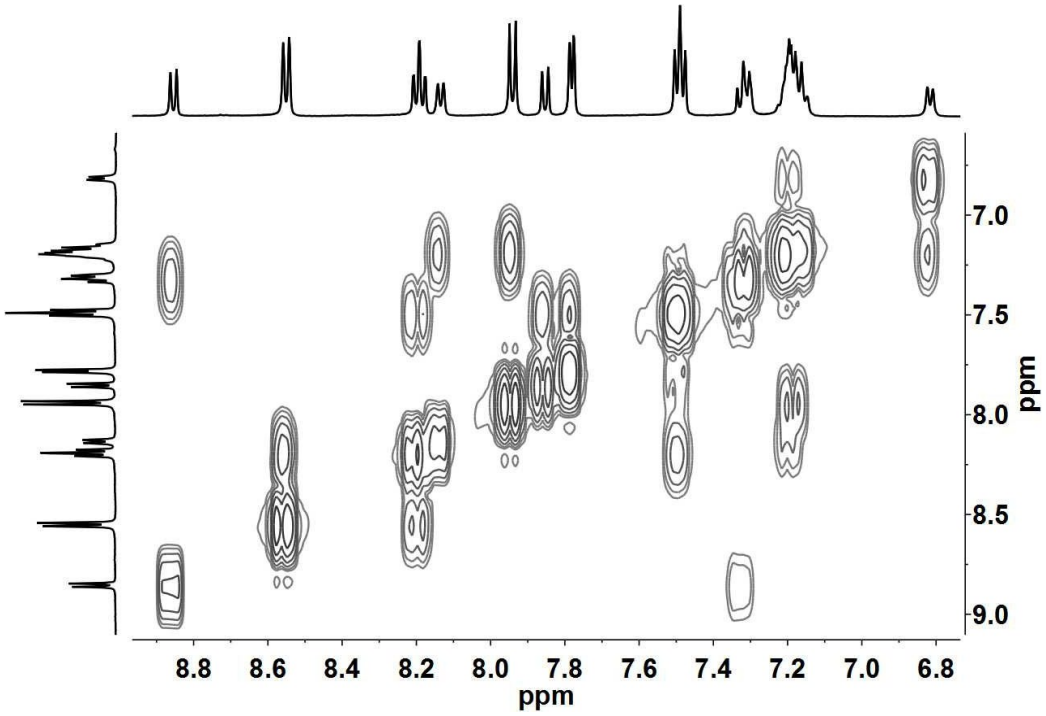

Fig. S5 The 2D ^{1}H–^{1}H COSY NMR spectrum of **1·PF$_6$** (500 MHz, DMSO-d_6). The signals from H-N$_{imidazole}$ were omitted for clarity.

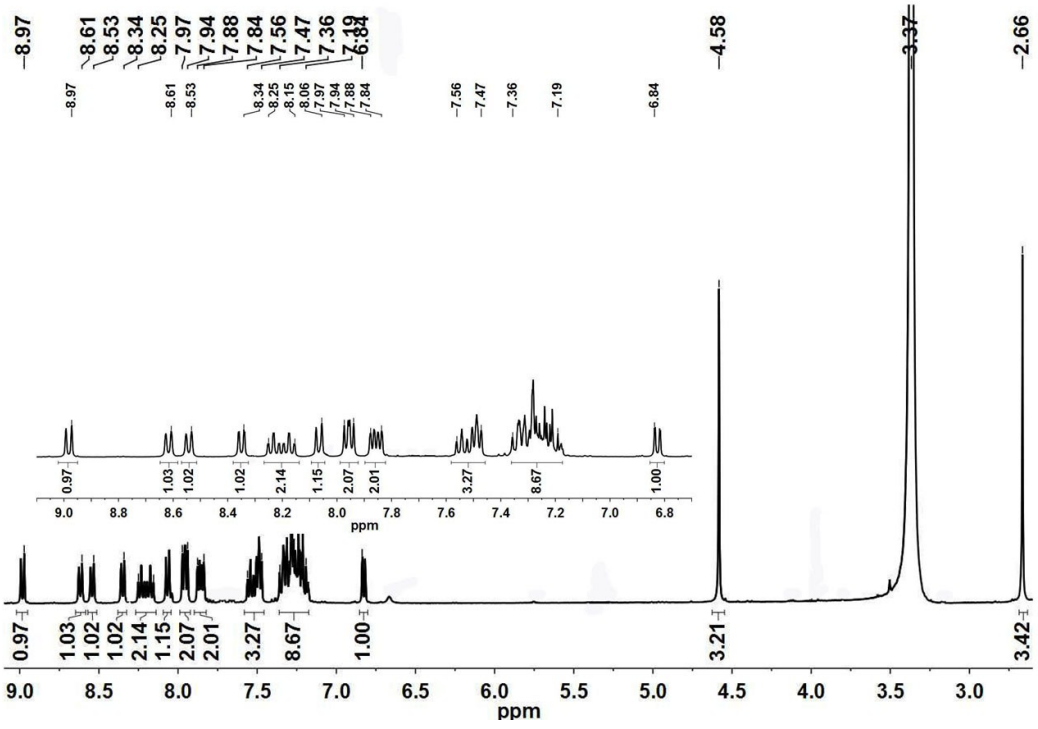

Fig. S6 ^{1}H NMR spectrum of **2·PF$_6$** (500 MHz, DMSO-d_6). The signals at 3.37 ppm is from H_2O.

Fig. S7 The 2D ^{1}H–^{1}H COSY NMR spectrum of **2·PF$_6$** (500 MHz, DMSO-d_6). The signals from CH_3 groups were omitted for clarity.

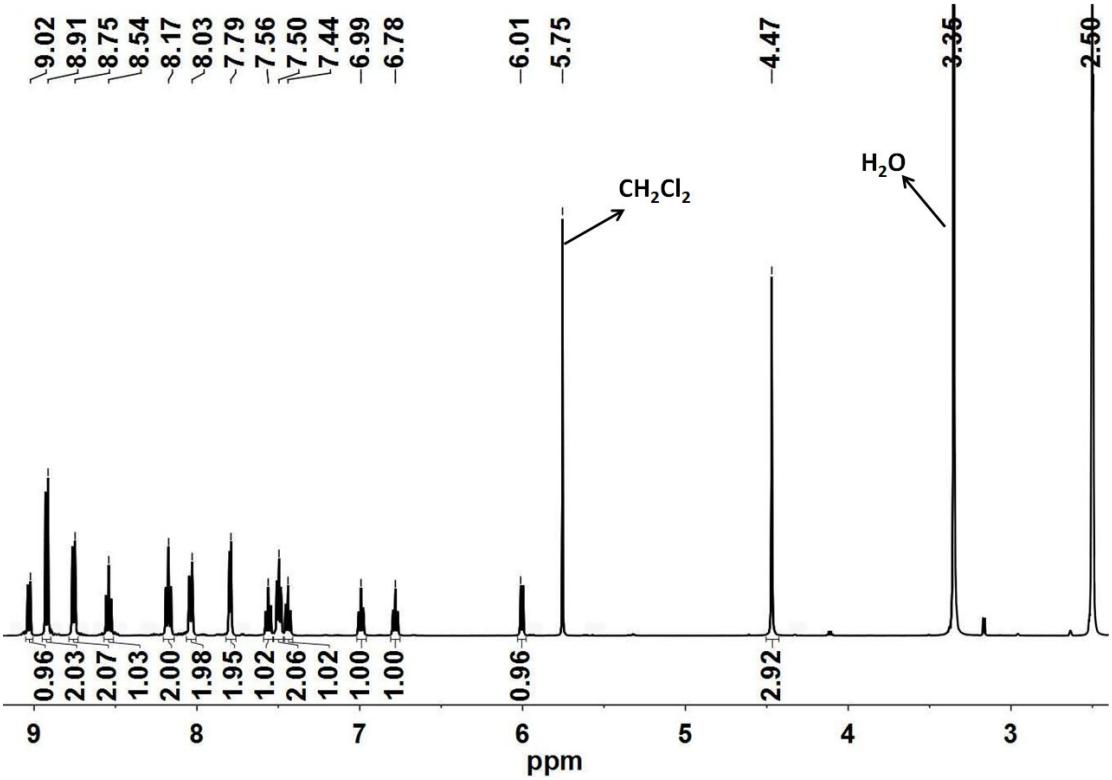

Fig. S8 ^{1}H NMR spectrum of **3·PF$_6$** (500 MHz, DMSO-d_6. The signals at 5.76 and 3.35 ppm are from CH_2Cl_2 and H_2O, respectively.

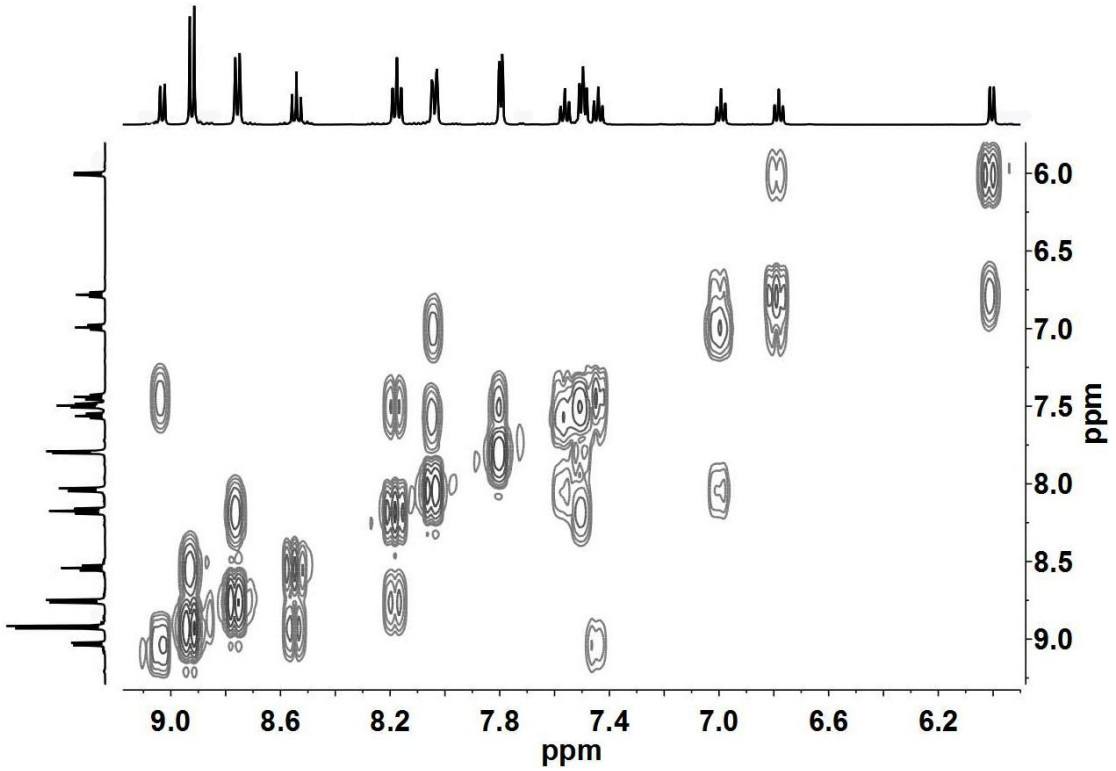

Fig. S9 The 2D ^{1}H–^{1}H COSY NMR spectrum of **3·PF$_6$** (500 MHz, DMSO-d_6).

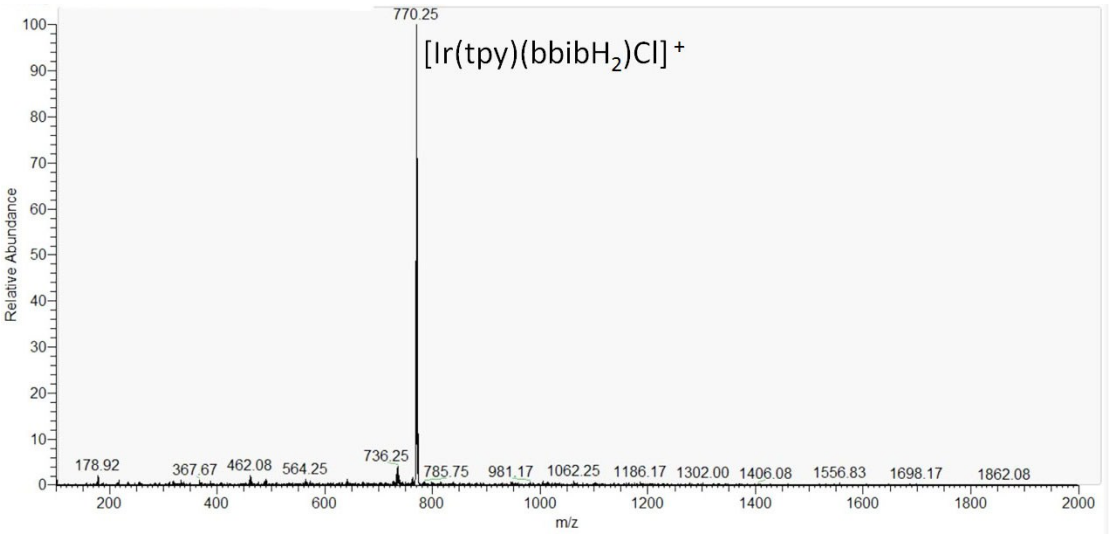

Fig. S10 Electrospray ionization mass spectrometry (ESI-MS) of **1·PF$_6$** in CH_2Cl_2-CH_3OH solution, showing a peak at 770.25.

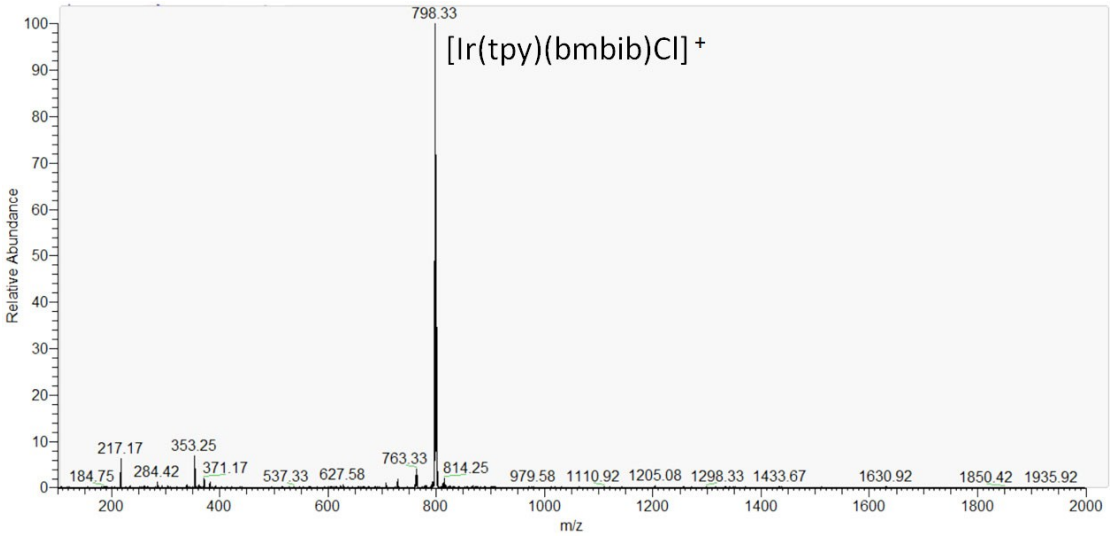

Fig. S11 Electrospray ionization mass spectrometry (ESI-MS) of **2·PF$_6$** in CH_2Cl_2-CH_3OH solution, showing a peak at 798.33.

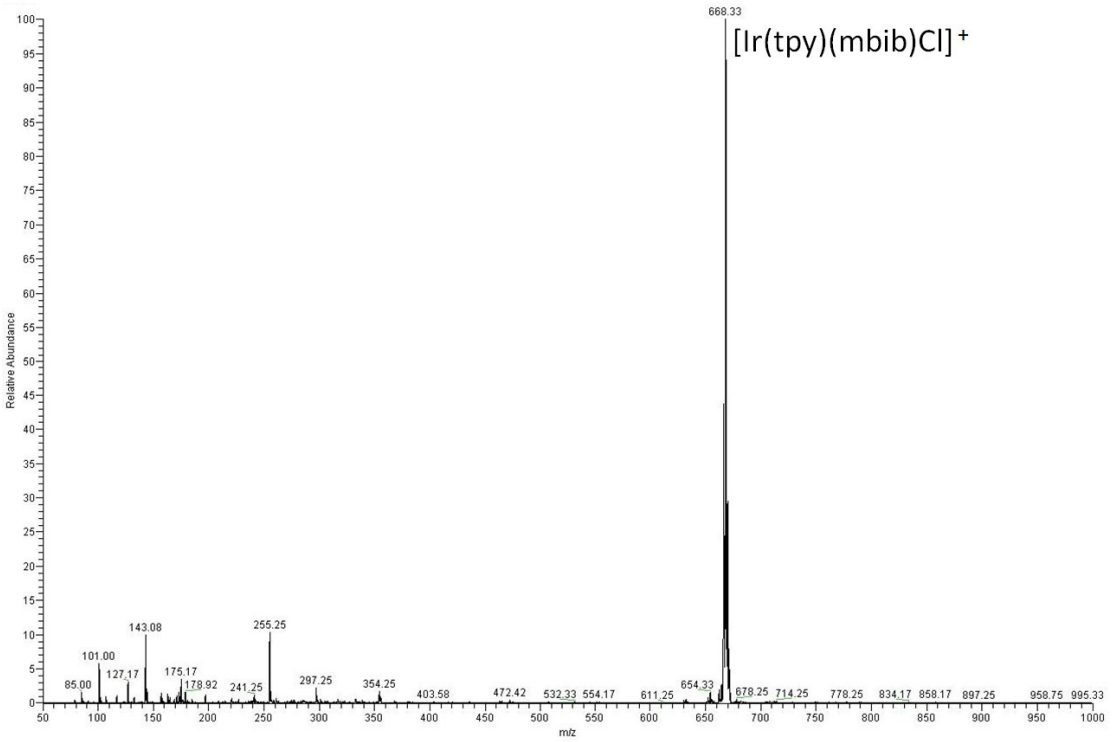

Fig. S12 Electrospray ionization mass spectrometry (ESI-MS) of **3·PF$_6$** in CH_2Cl_2-CH_3OH solution, showing a peak at 668.33.

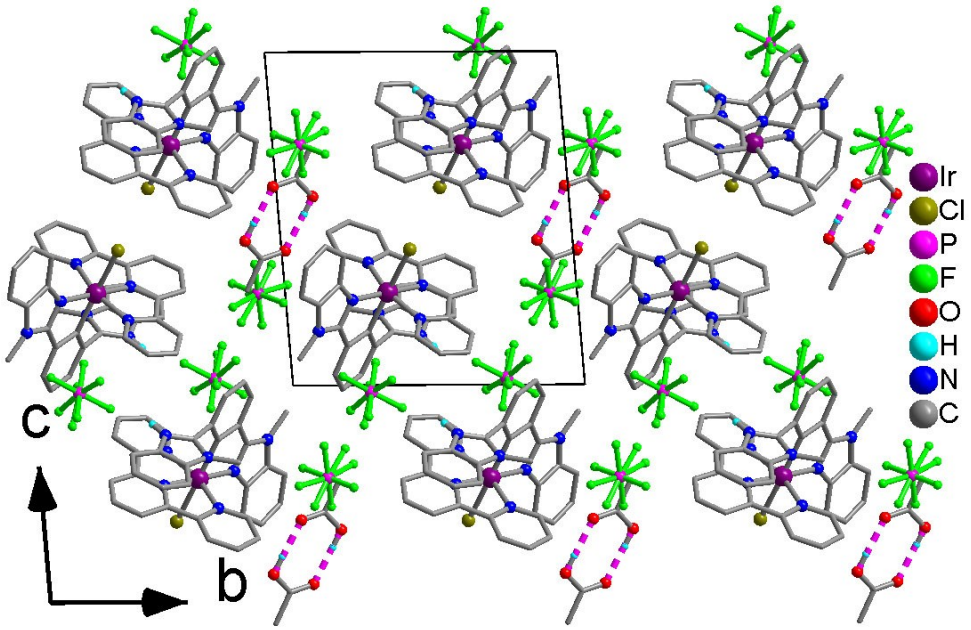

Fig. S13 The packing structure of $[\mathbf{2}H]^{2+}\cdot 2PF_6^-\cdot CH_3COOH$.

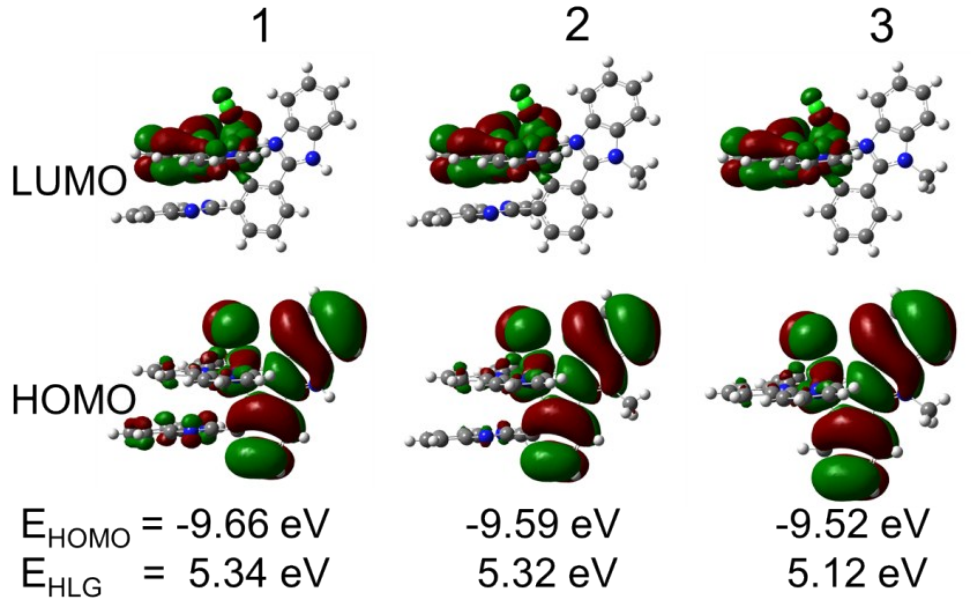

Fig. S14 Frontier molecular orbitals of the molecular structures of **1**, **2** and **3**. (isovalue = 0.01). Energies of HOMO and HOMO-LUMO gaps (HLGs) are given.

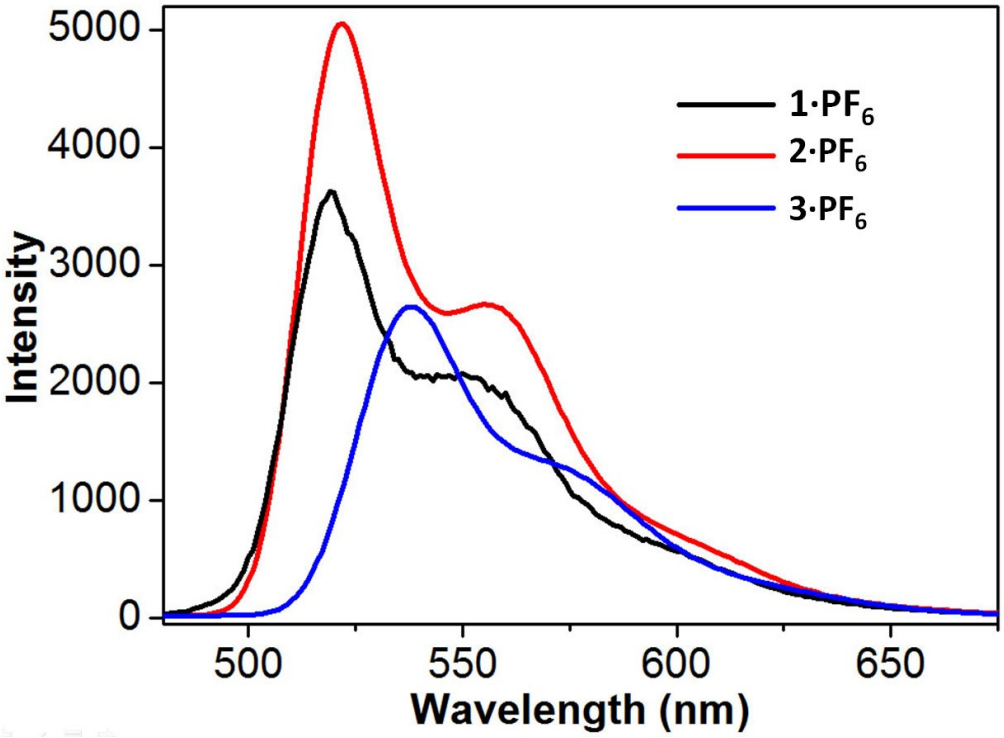

Fig. S15 Phosphorescence spectra of **1·PF$_6$**, **2·PF$_6$** and **3·PF$_6$** in EtOH-MeOH (v/v = 3/1) at 77 K (c = 1.0 × 10^{-4} M, λ_{ex} = 368 nm).

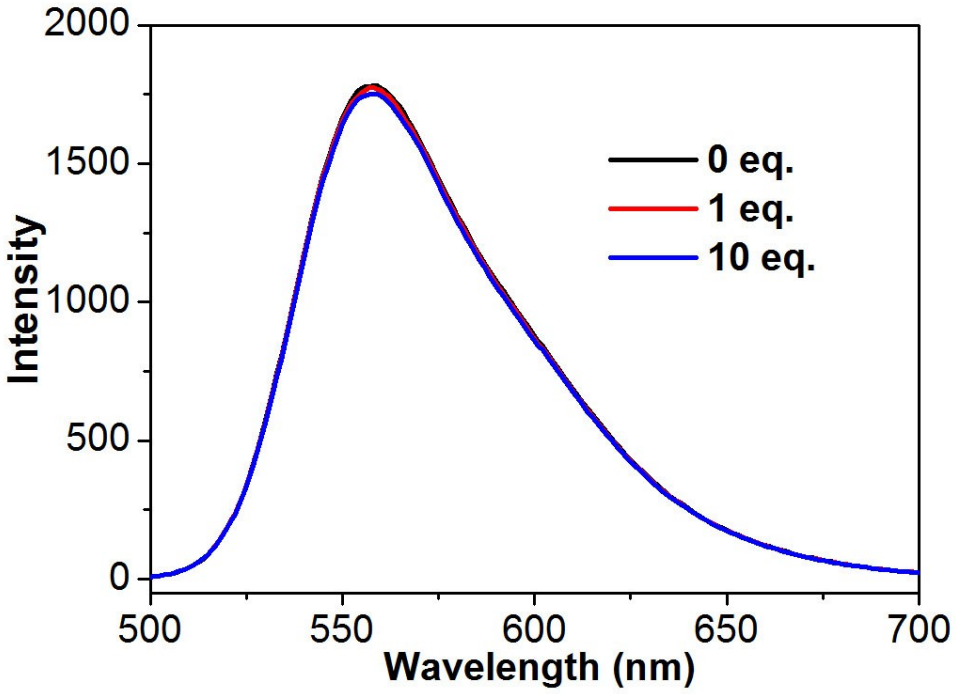

Fig. S16 Luminescence spectral changes of **3·PF$_6$** in CH_3CN (c = 1 × 10^{-4} M, λ_{ex} = 368 nm) upon adding TFA at room temperature.